Asian Journal of Chemistry; Vol. 27, No. 3 (2015), 889-894

ASIAN JOURNAL OF CHEMISTRY

http://dx.doi.org/10.14233/ajchem.2015.17385

Novel Method for Fabrication of Super-Hydrophobic Film on Magnesium Alloy and Consequent Anticorrosion Performance

LIYUAN MIN* and RUNHU ZHANG

Department of Chemical Engineering, Kunming Metallurgy College, Kunming 650033, P.R. China

*Corresponding author: E-mail: minliyuan_kmc@163.com

Received: 13 February 2014; *Accepted*: 5 May 2014; *Published online*: 19 January 2015; AJC-16691

A novel two-step dipping method has been proposed to fabricate super-hydrophobic film on magnesium alloy with hexamethylene-diisocyanate trimer (HDI trimer) and laurylamine. With this method, super-hydrophobic film, which is composed of HDI trimer-laurylamine biuret, can be fabricated on metal surface within 10 sec. The film morphologies and chemical compositions were investigated using scanning electron microscope and Fourier-transform infrared spectrophotometer. It is shown that rough micro-structure and low surface energy of biuret film confer super-hydrophobicity of resultant film. The concentrations of HDI trimer and laurylamine are investigated to determine their effects on wettability of film. Furthermore, the anticorrosion performance and mechanism of super-hydrophobic film to magnesium alloy in 3.5 % NaCl solution are studied with electrochemical measurements. It is proven that super-hydrophobic film can protect underlying magnesium alloy effectively and the air trapped in film is the main contributor for the barrier performance.

Keywords: Super-hydrophobic film, Magnesium alloy, Corrosion protection, Polarization curve.

INTRODUCTION

Magnesium alloys have been applied widely owing to their special advantages including low density, high strength to weight ratio, high dimensional stability, good electromagnetic shielding and damping characteristics and good machining and recycling ability, *etc*.[1-5]. Magnesium alloy, however, is easily corroded due to low standard potential, which aggravates the large-scale use of magnesium alloy[6,7].

Electrochemical corrosion is one of the main forms of corrosion in nature and aqueous medium is the essential factor for electrochemical corrosion process. Surface modification, which provides a barrier to erosion by aqueous medium, is an effective method for improving corrosion resistance of metal. Based on this theory, numerous methods, which include paint coating[8], sol-gel coating[9], conversion coating[10] and so on[11-15], have been proposed up to date.

Wettability to water reflects the affinity of solid surface to water. It is an important factor that should be considered for corrosion protection of metal. Generally, hydrophobic film presents better corrosion protection performance in comparison with hydrophilic film, because it can inhibit the penetration of aqueous solution into film and thus impede the formation of corrosion cell. Artificial super-hydrophobic surface, inspired from lotus leaf, is regarded as an effective corrosion protection method for its resistance to water contact[16-18]. Higher surface roughness and lower surface energy are two important factors for fabrication of super-hydrophobic surface[19,20]. Based on this theory, numerous methods have been proposed for artificial super-hydrophobic surface fabrication, including ultrasound irradiation[21], lithography[22] and so on[23,24]. Many drawbacks, however, exist for the application of super-hydrophobic film in industry, such as long fabricating time, requiring expensive equipments and complicated fabrication process. Thus, it is desired to propose a facial and time-saving method for super-hydrophobic film fabrication.

Herein, a novel two-step dipping method has been proposed to fabricate super-hydrophobic film on magnesium alloy surface. The fabrication process is facile and can be finished within 10 seconds. It does not require expensive reagents and complicated equipment. The origin of super-hydrophobic property of resultant film is clarified according to chemical composition and morphology analysis. Electrochemical measurements results demonstrate that super-hydrophobic film prepared on magnesium alloy surface can protect the substrate effectively.

EXPERIMENTAL

Magnesium alloy AZ31 (composition: 2.98 wt. % Al, 0.88 wt.% Zn, 0.38 wt.% Mn, 0.0135 wt.% Si, 0.001 wt.% Cu, 0.002 wt.% Ni, 0.0027 wt.% Fe and the rest is Mg) was used in this study. Sodium chloride, ethanol, acetic ether and laurylamine were obtained from Shanghai Chemical Reagent

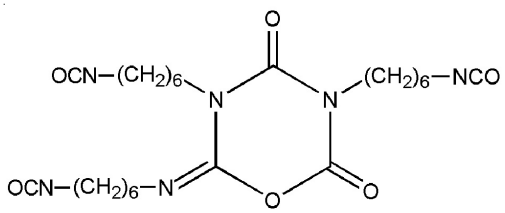

Scheme-I: Chemical structure of HDI trimer

Co., China. Hexamethylene-diisocyanate trimer (HDI trimer) was obtained from Bayer AG, Germany and its chemical structure is shown in **Scheme-I**.

Fabrication of hydrophobic/super-hydrophobic film: Magnesium alloy substrate was polished with SiC paper up to 2000 #, rinsed with deionized water and dried in air. After the pretreatment, the substrate was immersed in HDI trimer/acetic ether solution with concentration varying from 0.5 M to 0.02 M for 5 seconds and then it was transferred into laurylamine/acetic ether solution with concentration varying from 0.1 M to 0.004 M for 5 seconds. After that, the substrate was taken out, washed with acetic ether and dried in air. The diagram of dipping treatment is shown in Fig. 1.

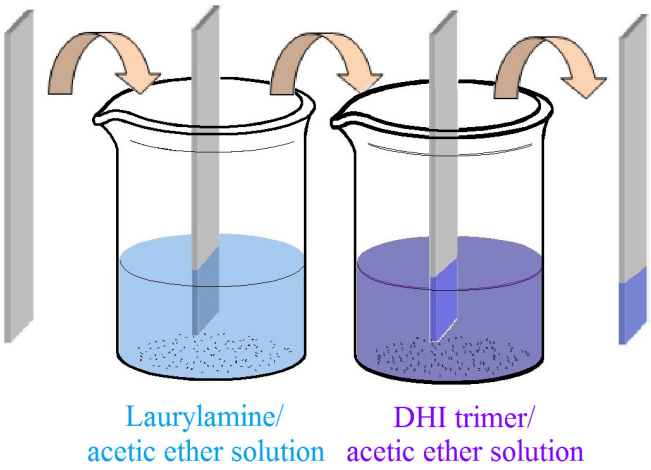

Fig. 1. Schematic diagram for the hydrophobic/super-hydrophobic film fabrication process

Characterization and tests: Wettability of film was characterized with a water drop volume of 10 μL using an optical contact angle meter (POWEREACH JC2000C1) at ambient temperature. Film morphology was characterized with FE-SEM (HITACHI S-4800) and film composition was characterized with FT-IR spectrum (Nicolet iSIO spectrometer). Optical images were obtained using a digital microscope system (HIROX KH-7700) to illustrate the 3-D topology of the bare and modified magnesium alloy specimens. The electrochemical experiments, including polarization curves and open circuit potential (E_{oc})-*t* curves, were carried out with a computer-controlled electrochemical system (CHI 706C, CH Instruments Inc.) at room temperature in 3.5 wt. % NaCl solution. They were performed in a three-electrode cell with a platinum electrode as counter electrode, bare magnesium alloy specimen/filmed magnesium alloy specimen as working electrode and a silver/silver chloride (Ag/AgCl) electrode as reference electrode. Polarization curves were recorded at a sweep rate of 1 mV s^{-1}.

RESULTS AND DISCUSSION

Composition of film: Fig. 2 presents FT-IR spectra of (a) laurylamine, (b) HDI trimer and (c) super-hydrophobic film in range of 4000-400 cm^{-1}. In cases of laurylamine (Fig. 2a) and HDI trimer (Fig. 2b), three peaks are observed at similar wavelengths and they are related to asymmetric vibration of -CH_2- at 2918 cm^{-1}, symmetric vibration of -CH_2- at 2853 cm^{-1} and bending vibration of -CH_2- at 1476 cm^{-1} [25,26], indicating the presence of -CH_2- group in both cases. This result is in conformity with the chemical structure of the two reagents (**Scheme-I**). A weak peak related to asymmetric vibration of -CH_3 at 2959 cm^{-1} can be observed in both cases of laurylamine (Fig. 2a) and super-hydrophobic film (Fig. 2c). It is indicated that the -CH_3 group exists in super-hydrophobic film and it certainly comes from laurylamine moiety. Noticeably, in comparison with the two reactants (laurylamine and HDI trimer), the typical bands for -NH_2 group of laurylamine (819 cm^{-1} in Fig. 2a) and -NCO group of HDI trimer (2270 cm^{-1} in Fig. 2b) disappear, whereas a new band corresponding to secondary amide group appears in super-hydrophobic film (1624 cm^{-1} in Fig. 2c). It can be inferred that the film is mainly composed of the material HDI trimer-laurylamine biuret from reaction shown in **Scheme-II**.

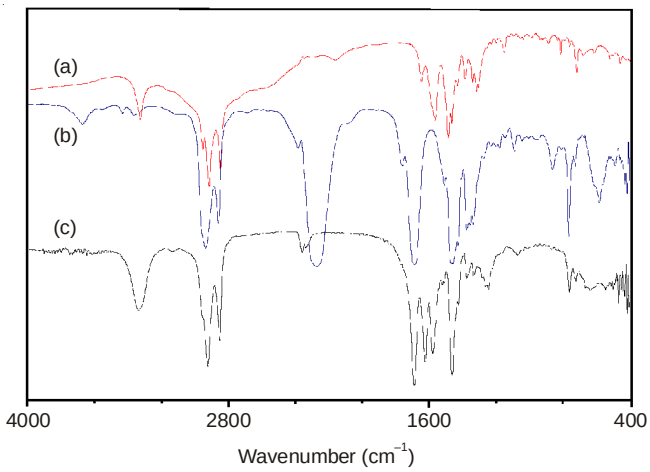

Fig. 2. FT-IR of (a) laurylamine, (b) HDI trimer and (c) super-hydrophobic film

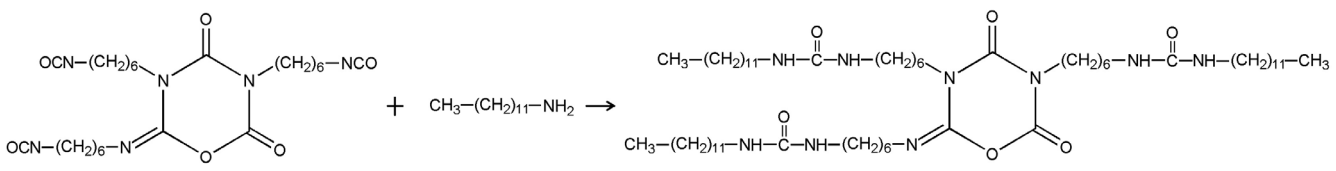

Scheme-II: Reaction equation between HDI trimer and laurylamine

Morphology and wettability: It is clear that film forms on magnesium alloy surface for the reaction between HDI trimer and laurylamine and concentrations of HDI trimer and laurylamine might be two important factors that influence morphology of film, which can further affect film wettabiliy. In this work, the influences of reagents (HDI trimer and laurylamine) concentration on film wettability were investigated. Figs. 3a-f present variation of morphology and wettability of film fabricated with HDI concentration ranging from 0.02 to 0.5 M (laurylamine concentration is fixed as 0.1 M). In the case of low concentration of HDI trimer (0.02 M), film can be hard to be detected on alloy surface under low magnification (Fig. 3a) and dispersive cluster structures can be observed under high magnification (Fig. 3b). The modified alloy surface presents hydrophilic property with contact angle of 83.7 ± 3º for the low coverage of film over alloy surface (Fig. 3a). Once the concentration of HDI trimer increases to 0.1 M, a discontinuous film can be easily observed on magnesium alloy surface (Figs. 3c, d) and the modified magnesium alloy surface presents hydrophobic property with water contact angle of 135.1±3º. In case that HDI trimer concentration increases to 0.5 M, a continuous film forms over alloy surface and it presents super-hydrophobic property with contact angle of 156.7±3º (Fig. 3e). It is clear that the film is composed of island-like structures with hundreds of micrometers scale. From its enlarged picture (Fig. 3f), it can be observed that the island-like structure presents wrinkle-like secondary structure, which provides nano-scale roughness on top of the micrometer sized island-like structures. Such particle organization results in a hierarchical microscale-to-nanoscale roughness, which is known to produce super-hydrophobicity on natural and artificial surfaces. Figs. 3e-h present variation of morphologies and wettability of film fabricated with concentration ranging from 0.1 to 0.004 M (HDI trimer concentration is fixed as 0.5 M). In case that laurylamine concentration decreases from 0.1 M to 0.02 M, the wettability of film transfers from super-hydrophobic property to hydrophobic property with contact angle of 120.8 ± 3º for the discontinuity of resultant film (Fig. 3g), though the two kinds of film present similar secondary micro-structure (Fig. 3h). When the laurylamine concentration further decreases to 0.004 M, the film gets thinner (Fig. 3j) and the water contact angle on its surface decreases to 108.8 ± 3º for the decrease of film coverage (Fig. 3i).

Formation process of film: As shown in Fig. 1, after the magnesium alloy is pulled out of HDI trimer/acetic ether solution, a thin HDI trimer/acetic ether solution film sticks over its surface. Then, the specimen is transferred into laurylamine/acetic ether solution, in which, laurylamine molecule reacts with HDI trimer immediately to form HDI trimer-laurylamine biuret film over magnesium alloy surface. Basing on this reaction mechanism, it is not difficult to understand that higher regent concentration is helpful for intensifying hydrophobic property of resultant film by creating thick and continuous film with rough structure.

In order to clarify the origin of super-hydrophobic property of film (Figs. 3e,f), optical photography technique is employed to reveal the difference of topology between bare and filmed magnesium alloy in a wide scope fashion. From 3D view of bare magnesium alloy (Fig. 4a), it can be found that bare

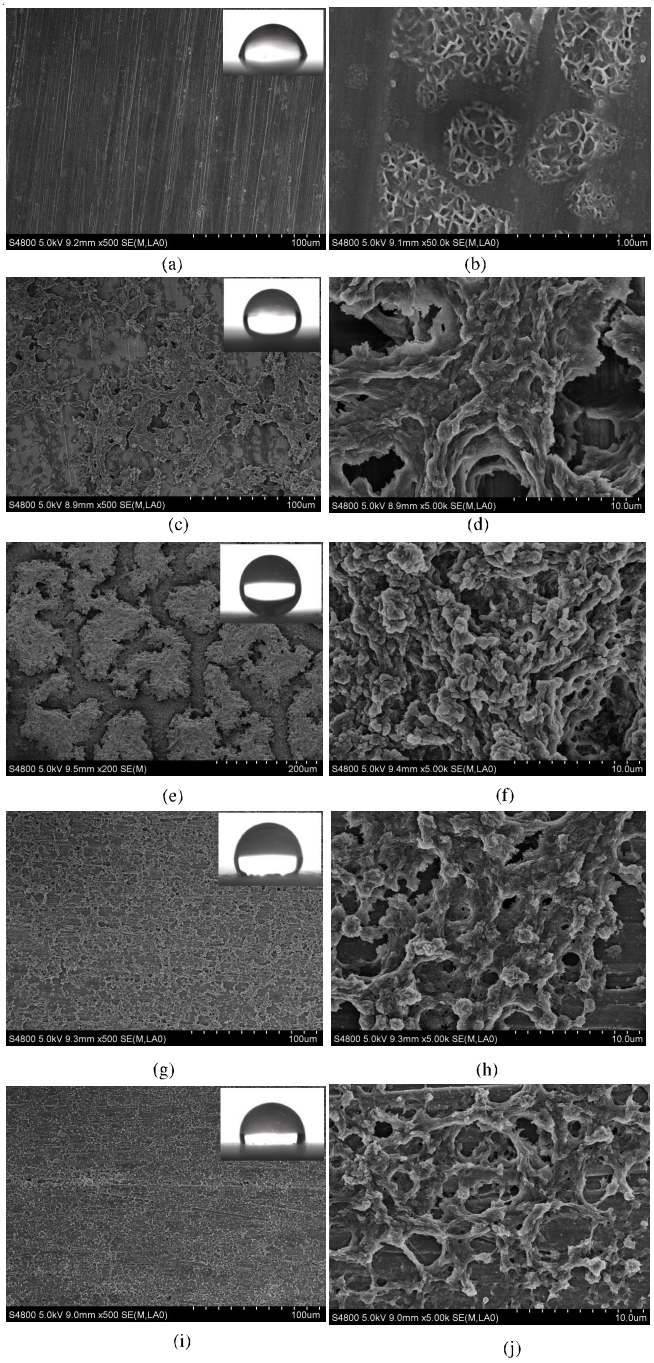

Fig. 3. Variation of film morphology and wettability with concentration of HDI trimer and laurylamine

magnesium alloy surface is relatively smooth within the test scope. From the height variation of a randomly selected cross section of bare magnesium alloy (Fig. 4b), it is clear that the height variation of bare magnesium alloy within the selected zone is less than 8 μm. Figs. 4c, d present the results of magnesium alloy covered with super-hydrophobic film, which is fabricated by immersion in HDI trimer/acetic ether solution (0.5 M) and laurylamine/acetic ether solution (0.1 M) in succession. Similar with the morphology captured with SEM (Fig. 3e), relatively independent island-like structures can be found on filmed magnesium alloy surface (Fig. 4c). The height variation of a randomly selected cross section of surface within the selected zone is more than 40 μm (Fig. 4d). It is indicated

that roughness of modified magnesium alloy surface increases for the formation of film. Furthermore, as proven in **Scheme-II**, the hydrocarbon chain of HDI trimer-laurylamine biuret can provide low surface energy to modified magnesium alloy surface. Once a water droplet is placed on the modified magnesium alloy surface, it can hard to penetrate into the rough structure of film for capillary action and it connects with rough surface through the interface composed of both solid/air and solid/liquid interfaces. The air trapped in the rough structure intensifies the hydrophobic property of film. According to this result, Cassie mode is employed to illuminate the super-hydrophobic property of film. Assuming that the water contact angle for air is 180°, the apparent contact angle (θ) can be expressed as follows[27,28]:

$$\cos \theta_r = f_1 \cos \theta - f_2 \quad (1)$$

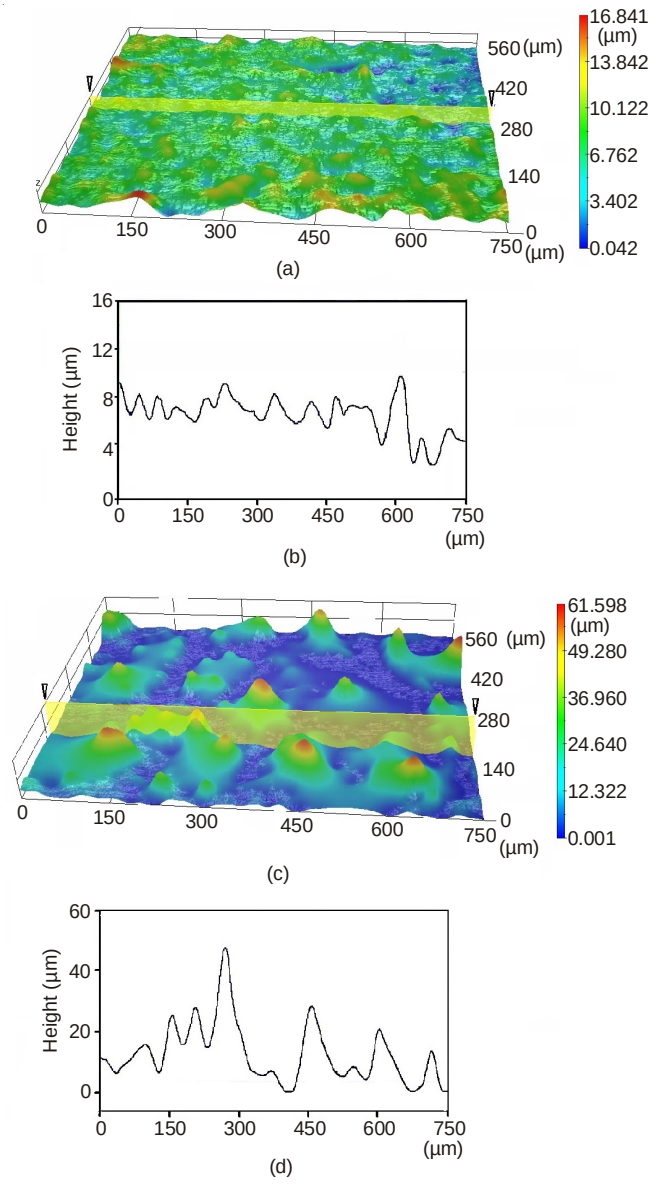

Fig. 4. Optical images of (a, b) bare magnesium alloy and (c, d) magnesium alloy modified with super-hydrophobic film. (a, c) 3-D image of the topology, (b, d) cross-sectional view showing the surface height variation

In eqn. 1, f_1 and f_2 are the fractions of the film surface and air in contact with water; θ_r and θ are the contact angles on the rough and smooth surfaces, respectively. According to previous reports[29,30], the contact angle of solid surface (HDI trimer-laurylamine biuret) is generally in the range 133°-115° when $-CH_3$ group exposed to air. The f_1 value of the super-hydrophobic film with a water contact angle of 156.7° (Fig. 3e) is 0.134 and the air fraction is 0.866. According to the calculation, it is clear that the high air fraction results in the super-hydrophobic property of the filmed magnesium alloy for the rough structure of film.

Dynamic wettability of film is an important aspect of wettability of solid surface. The behaviour of water droplet on the magnesium alloy modified with super-hydrophobic film is captured with a speed of 25 frames/s. As shown in Fig. 5, after a water droplet falls onto the modified magnesium alloy surface with a low declining angle (~ 5°), it cannot stick on the film but rolls off instead, demonstrating that the super-hydrophobic film presents a dynamic wettability with rolling angle less than 5°. In order to explain this behaviour, the adhesion of a water droplet on modified alloy surface is tested with the method reported by Gao *et al.*[31]. As shown in Fig. 6, the magnesium alloy modified with super-hydrophobic film is lifted to contact the droplet suspending on the outlet of a micro-syringe. After that, the specimen is moved down from the droplet. Although deformation occurs during this process, the water droplet can completely depart from the filmed alloy surface. It is indicated that the surface has low apparent water adhesion to the water droplet and this can be attributed to the low apparent contact area between water droplet and super-hydrophobic film and the further reduction of contact area for the existence of air in film as well. As a result, water droplet can roll off super-hydrophobic film easily (Fig. 5).

Fig. 5. Behavior of water droplet on super-hydrophobic film with a declining angle of less than 5°

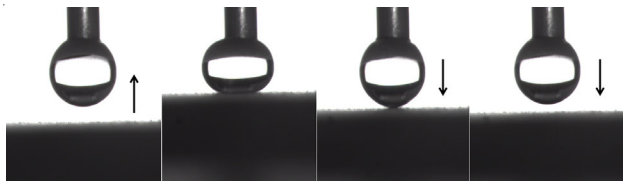

Fig. 6. Adhesion interaction between water droplet and the super-hydrophobic alloy surface. A water droplet is suspended on the outlet of a micro-syringe, and the beneath substrate is the magnesium alloy covered with super-hydrophobic film. (The arrows represent the moving direction of the substrate)

Corrosion protection performance of super-hydrophobic film: Before we test the corrosion protection performance of super-hydrophobic film to aqueous corrosive medium, the existence state of super-hydrophobic film in aqueous solution should be clarified first. As is known, air trapped in rough structure of film is an essential factor for super-hydrophobic property of film in atmospheric condition. The super-hydrophobic property of film will vanish in case that air is driven out of film. Similarly, existence of air in rough structure of film is also an evidence for maintaining super-hydrophobic

property of film in aqueous solution. After the magnesium alloy modified with super-hydrophobic film is immersed in 3.5 % NaCl solution, its surface is bright when viewed from the side. This phenomenon proves that the film can presents super-hydrophobic property in aqueous solution according the theory of total reflection in optics. In details, the super-hydrophobic film traps air in rough surfaces and the liquid forms a convex surface between the interface of liquid and air for the capillary. Air is optically a thinner medium for water because it presents a lower refractive index. When light transfers from the water to the interface of air with an incidence angle larger than the critical angle, the refraction light vanishes and the light is completely reflected[32].

To clarify the corrosion protection mechanism of super-hydrophobic film to the underlying magnesium alloy, it is effective to compare corrosion protection performance of super-hydrophobic film before and after air is driven out of rough structure of film. For this aim, a deaeration process for super-hydrophobic film immersed in aqueous solution should be first designed[32]. Our experiment indicates that ethanol can spread over the resultant super-hydrophobic film, indicating that ethanol can penetrate into rough structure of super-hydrophobic film and replace the air film. Thus, a deaeration method for super-hydrophobic film can be designed based on this experiment result. Firstly, the specimen covered with super-hydrophobic film is immersed in ethanol for 5 min to facilitate the replacement of air in film by ethanol. Then, the specimen wetted by ethanol is transferred immediately into 3.5 wt. % NaCl solution. After this step, the ethanol in the rough structure of super-hydrophobic film can be replaced gradually by NaCl solution because of the completely mutual solubility of ethanol in water. Therefore, the air trapped in the film can be driven out and deaerated super-hydrophobic film can be obtained through this method. After this deaeration process, the deaerated super-hydrophobic film is no longer as bright as the super-hydrophobic film when viewed from side, proving that the contact mode between NaCl solution and super-hydrophobic film changes (Fig. 7). To avoid air being trapped in the film again, the electrochemical experiments for deaerated super-hydrophobic film is carried out after the above-mentioned deaeration process without taking the specimen out of NaCl solution.

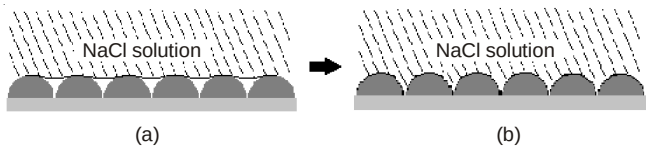

Fig. 7.Contact modes between NaCl solution and super-hydrophobic film: (a) before and (b) after deaeration process

Fig. 8 shows the E_{oc}-*t* curves of bare magnesium alloy specimen, magnesium alloy covered with super-hydrophobic film and magnesium alloy specimen covered with deaerated super-hydrophobic film in 3.5 % NaCl solution. The E_{oc} of bare magnesium alloy specimen is around -1.35 V. Noticeably, E_{oc} of magnesium alloy covered with super-hydrophobic film is unstable within the testing interval, suggesting the poor electro-conductive property of the super-hydrophobic film for the trapped air. After air is driven out, E_{oc} of sample covered with deaerated super-hydrophobic film gets stable and falls down to about -1.4 V and its E_{oc} - *t* curve almost coincides with that of bare magnesium alloy specimen. It is implied that the deaeration weakens the corrosion protection performance of the super-hydrophobic film to substrate.

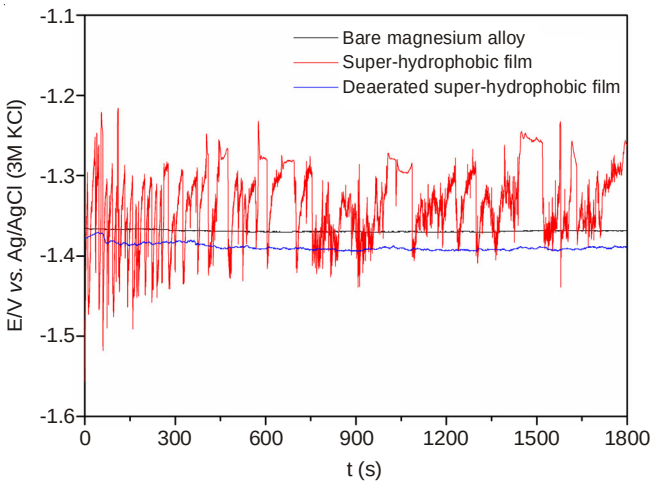

Fig. 8. E_{oc}- *t* curves of bare magnesium alloy, magnesium alloy with super-hydrophobic film and magnesium alloy with deaerated super-hydrophobic film in 3.5 wt. % NaCl solution

Fig. 9 shows polarization curves of bare magnesium alloy, magnesium alloy covered with super-hydrophobic film and magnesium alloy covered with deaerated super-hydrophobic film in 3.5 % NaCl solution. The cathodic reaction in the polarization curve corresponds to the evolution of the hydrogen and the anodic polarization curve is the most important features related to the corrosion resistance of film. In the presence of super-hydrophobic film, the anodic and cathodic polarization current densities are reduced for more than five and four orders of magnitude, respectively and the polarization current density maintains less than 10^{-7} A cm^{-2} within the testing potential ranging from -1.3 to -1.6 V. It is proven that super-hydrophobic film can present effective barrier effect to the underlying magnesium alloy. By comparing results of specimen covered

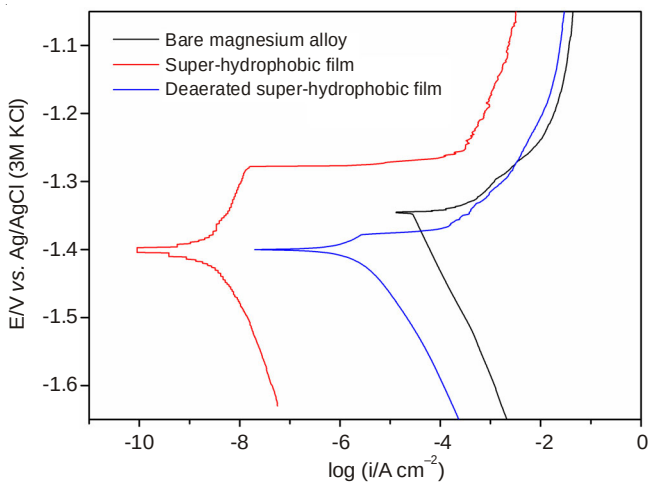

Fig. 9. Polarization curves of bare magnesium alloy, magnesium alloy with super-hydrophobic film and magnesium alloy with deaerated super-hydrophobic film in 3.5 wt. % NaCl solution

with super-hydrophobic film before and after deaeration, it is clear that the polarization current density of filmed magnesium alloy increases conspicuously after the air is driven out. The cathodic current density of filmed specimen after deaeration can only be reduced for about two orders of magnitude in comparison with that of bare specimen and its anodic current density is almost the same with that bare specimen. It is indicated that the air trapped in film plays an essential role in corrosion protection performance of super-hydrophobic film to underlying magnesium alloy for its insulation. In addition to acting as a "frame"to trap air, the film itself can inhibit the cathodic reaction of magnesium alloy to some extent.

Conclusion

A novel two-step dipping method has been proposed to fabricate super-hydrophobic film on magnesium alloy surface with HDI trimer and amine. With this method, super-hydrophobic film can be fabricated on magnesium alloy surface within 10 sec. It is found that hierarchical microscale-to-nanoscale roughness and low surface energy of film confer super-hydrophobicity of resultant film. Water droplet can roll off the resultant super-hydrophobic film easily for the low attraction between water droplet and super-hydrophobic film. The concentrations of HDI trimer and amine are investigated to determine their effects on wettability of film. High concentration of reactants is proven to be helpful for constructing a continuous film with intensified hydrophobicity. Electrochemical measurements indicate that the polarization current density can be reduced for more than four orders of magnitude in the presence of super-hydrophobic film. Air trapped in film is the main contributor to the effective corrosion protection performance of super-hydrophobic film and the film itself can help to inhibit corrosion process by suspending cathodic reaction. The method proposed for super-hydrophobic film fabrication is facial and time-saving and it will hopefully be applied for corrosion protection of magnesium in industries.

REFERENCES

1. Z. Wang, Q. Li, Z. She, F. Chen, L. Li, X. Zhang and P. Zhang, *Appl. Surf. Sci*., **271**, 182 (2013).
2. X. Lu, Y. Zuo, X. Zhao, Y. Tang and X. Feng, *Corros. Sci*., **53**, 153 (2011).
3. A. Abdal-hay, M. Dewidar and J.K. Lim, *Appl. Surf. Sci*., **261**, 536 (2012).
4. X. Ye, S. Cai, Y. Dou, G. Xu, K. Huang, M. Ren and X. Wang, *Appl. Surf. Sci*., **259**, 799 (2012).
5. Y. Chen, B.L. Luan, G.L. Song, Q. Yang, D.M. Kingston and F. Bensebaa, *Surf. Coat. Technol*., **210**, 156 (2012).
6. G.L. Song, *Electrochim. Acta*, **55**, 2258 (2010).
7. A. Pardo, S. Merino, M.C. Merino, I. Barroso, M. Mohedano, R. Arrabal and F. Viejo, *Corros. Sci*., **51**, 841 (2009).
8. Y. Zhang, Y. Shao, T. Zhang, G. Meng and F. Wang, *Prog. Org. Coat*., **76**, 804 (2013).
9. H. Wang, R. Akid and M. Gobara, *Corros. Sci*., **52**, 2565 (2010).
10. A.S. Hamdy and D.P. Butt, *Electrochim. Acta*, **108**, 852 (2013).
11. Y. Zhao, M.I. Jamesh, W.K. Li, G. Wu, C. Wang, Y. Zheng, K.W.K. Yeung and P.K. Chu, *Acta Biomater*., **10**, 544 (2014).
12. T. Ishizaki, Y. Masuda and K. Teshima, *Surf. Coat. Technol*., **217**, 76 (2013).
13. F. Brusciotti, D.V. Snihirova, H. Xue, M.F. Montemor, S.V. Lamaka and M.G.S. Ferreira, *Corros. Sci*., **67**, 82 (2013).
14. X. Guo, K. Du, Q. Guo, Y. Wang, F. Wang and F. Wang, *Corros. Sci*., **76**, 129 (2013).
15. I.A. Kartsonakis, A.C. Balaskas, E.P. Koumoulos, C.A. Charitidis and G. Kordas, *Corros. Sci*., **65**, 481 (2012).
16. R. Qiu, D. Zhang and P. Wang, *Corros. Sci*., **66**, 350 (2013).
17. P. Wang, D. Zhang, R. Qiu and B. Hou, *Corros. Sci*., **53**, 2080 (2011).
18. P. Wang, D. Zhang, R. Qiu, J. Wu and Y. Wan, *Corros. Sci*., **69**, 23 (2013).
19. X. Feng, L. Feng, M. Jin, J. Zhai, L. Jiang and D. Zhu, *J. Am. Chem. Soc*., **126**, 62 (2004).
20. T. Sun, G. Wang, L. Feng, B. Liu, Y. Ma, L. Jiang and D. Zhu, *Angew. Chem. Int. Ed*., **43**, 357 (2004).
21. M.E. Yazdanshenas and M. Shateri-Khalilabad, *Ind. Eng. Chem. Res*., **52**, 12846 (2013).
22. H.J. Choi, S. Choo, J.H. Shin, K.I. Kim and H. Lee, *J. Phys. Chem. C*, **117**, 24354 (2013).
23. S.G. Lee, D.S. Ham, D.Y. Lee, H. Bong and K. Cho, *Langmuir*, **29**, 15051 (2013).
24. J. Ou, W. Hu, M. Xue, F. Wang and W. Li, *ACS Appl. Mater. Interfaces*, **5**, 3101 (2013).
25. G. Fonder, F. Laffineur, J. Delhalle and Z. Mekhalif, *J. Colloid Interf. Sci*., **326**, 333 (2008).
26. M.W. Tsao, J.F. Rabolt, H. Schönherr and D.G. Castner, *Langmuir*, **16**, 1734 (2000).
27. X.J. Feng and L. Jiang, *Adv. Mater*., **18**, 3063 (2006).
28. P. Wang, R. Qiu, D. Zhang, Z. Lin and B. Hou, *Electrochim. Acta*, **56**, 517 (2010).
29. M. Schem, T. Schmidt, J. Gerwann, M. Wittmar, M. Veith, G.E. Thompson, I.S. Molchan, T. Hashimoto, P. Skeldon, A.R. Phani, S. Santucci and M.L. Zheludkevich, *Corros. Sci*., **51**, 2304 (2009).
30. Cui Wang Xiao Su Chen. Z. Cui, Q. Wang, Y. Xiao, C. Su and Q. Chen, *Appl. Surf. Sci*., **254**, 2911 (2008).
31. X.F. Gao, X. Yao and L. Jiang, *Langmuir*, **23**, 4886 (2007).
32. P. Wang, D. Zhang and R. Qiu, *Corros. Sci*., **54**, 77 (2012).